Biosensors and Bioelectronics 39 (2013) 70–75

Contents lists available at SciVerse ScienceDirect

Biosensors and Bioelectronics

journal homepage: www.elsevier.com/locate/bios

A simple electrochemical approach to fabricate a glucose biosensor based on graphene–glucose oxidase biocomposite

Binesh Unnikrishnan, Selvakumar Palanisamy, Shen-Ming Chen *

Electroanalysis and Bioelectrochemistry Laboratory, Department of Chemical Engineering and Biotechnology, National Taipei University of Technology, No. 1, Section 3, Chung-Hsiao East Road, Taipei 106, Taiwan, ROC

ARTICLE INFO

Article history:
Received 17 March 2012
Received in revised form
19 June 2012
Accepted 21 June 2012
Available online 1 July 2012

Keywords:
Glucose oxidase
Immobilization
Reduced graphene oxide
Biosensor
Amperometry
Electrochemical reduction

ABSTRACT

We report a simple electrochemical approach for the immobilization of glucose oxidase (GOx) on reduced graphene oxide (RGO). The immobilization of GOx was achieved in a single step without any cross linking agents or modifiers. A simple solution phase approach was used to prepare exfoliated graphene oxide (GO), followed by electrochemical reduction to get RGO–GOx biocomposite. The direct electrochemistry of GOx was revealed at the RGO–GOx modified glassy carbon electrode (GCE). The electrocatalytic and electroanalytical applications of the proposed film were studied by cyclic voltammetry (CV) and amperometry. It is notable that the glucose determination has been achieved in mediator-free conditions. RGO–GOx film showed very good stability, reproducibility and high selectivity. The developed biosensor exhibits excellent catalytic activity towards glucose over a wide linear range of 0.1–27 mM with a sensitivity of 1.85 $\mu A\,mM^{-1}\,cm^{-2}$. The facile and easy electrochemical approach used for the preparation of RGO–GOx may open up new horizons in the production of cost-effective biosensors and biofuel cells.

1. Introduction

Immobilizing enzymes efficiently on electrode surface is one of the most challenging tasks in a biosensor fabrication. Among the various enzymes, glucose oxidase (GOx) has received considerable importance in real-time glucose monitoring and biofuel cells related applications, due to its high selectivity to glucose. The two major limitations in immobilizing GOx on solid electrodes are: the poor electrical communication between the active site of the enzyme and the electrode, and enzyme leaching (Jody et al., 2007; Yang et al., 2003). To date, several methods have been employed to effectively immobilize GOx on the electrode surface. Entrapping or covalently immobilizing GOx in stable matrices including nano and mesostructured metal oxides (Cao et al., 2008; Fang et al., 2011), metal nanoparticles (Bharathi and Nogami, 2001; Baby et al., 2010), conducting polymers (Ekiz et al., 2010; Foulds et al., 1986; Alwarappan et al., 2010a), mesostructured silica (Blin et al., 2005), sol–gel matrix (Jia et al., 2007; Chen et al., 1998), carbon nanotubes (Lin et al., 2004; Periasamy et al., 2011), graphene (Shan et al., 2009; Kang et al., 2009; Zhou et al., 2010), etc., leads to the enhanced electron transfer and improved enzyme stability (Alwarappan et al., 2009, 2010b). Recently, Fu et al. (2011) demonstrated the use of metal-organic coordination polymers as a suitable immobilization matrix for GOx. Besides, GOx immobilized on conducting polymer/metal oxide composite (Xian et al., 2010) also exhibits enhanced direct electron transfer. All these findings reveal that choosing an immobilization matrix with good electrical conductivity, stability, and antifouling property is mandatory for biosensor applications.

Graphene is an inexpensive material with good mechanical, electrical and thermal properties (Novoselov et al., 2004; Geim and Novoselov, 2007) and it has perceived considerable attention recently. It has large surface area to volume ratio and good biocompatibility. Owing to the aforementioned properties, graphene is a potential matrix for electrochemical biosensors (Kuila et al., 2011). However, graphene sheets tend to form graphite by restacking (Li et al., 2008) due to the van der Waals force of attraction. In addition, dispersion of graphene in aqueous media is difficult due to its hydrophobic nature. So far, versatile strategies have been employed by several research groups to produce large yield and high-electronic quality graphene (Gengler et al., 2010; Shen et al., 2009). Though the chemical exfoliation method is much preferred for the large scale production of graphene sheets (Song et al., 2012), as-produced graphene sheets are not good enough for nanoelectronics applications (Guo et al., 2009). As an alternative, the electrochemical reduction method is more green (without using any toxic solvents), cost-effective and it is more suitable for preparing less defective graphene sheets.

Till date, numerous strategies have been successfully employed for immobilizing GOx efficiently on graphene (Wu et al., 2010),

* Corresponding author. Tel.: +886 2270 17147; fax: +886 2270 25238.
E-mail address: smchen78@ms15.hinet.net (S.-M. Chen).

0956-5663/$ - see front matter © 2012 Elsevier B.V. All rights reserved.
http://dx.doi.org/10.1016/j.bios.2012.06.045

graphene composite modified electrodes (Liu et al., 2011; Yang et al., 2010), graphene nanosheets, carbon nanospheres (Yin et al., 2011), etc. RGO modified electrode also have been employed. For instance, Wang et al. (2009a) demonstrated the immobilization of glucose oxidase on electrochemically reduced graphene oxide. In their approach, a single-layer GO was adsorbed on 3-aminopropyl-triethoxysilane modified electrode, then electrochemically reduced to RGO, electrografted with poly-N-succinimidyl acrylate and finally the GOx molecules were cross-linked through covalent bonding. However, this sort of approach is rather time consuming and it involves tedious enzyme immobilization procedures. On the other hand, Wang et al. (2003) synthesized a carbon nanotube (CNT) based biocomposite without any binders by dispersing CNT in GOx solution to construct an amperometric glucose biosensor. In most of the cases the immobilization methods involve many steps and need modifiers. However, to our knowledge no reports are available for the one step preparation of GO–GOx biocomposite without any cross-linkers or modifiers. The presence of oxygen functionalities on GO surface is much helpful for cross-linking and/or entrapping the enzyme (Liu et al., 2010). In the present study, we prepared GO–GOx biocomposite in one step, short time (with the aid of 30 min sonication) through the solution phase approach. The as-obtained GO–GOx biocomposite was electrochemically reduced to RGO–GOx and its electroanalytical applications towards the glucose determination have been studied in detail.

2. Experimental

2.1. Apparatus

The cyclic voltammetric experiments were carried out with a CHI 750A model electrochemical workstation. Amperometric experiments were carried out by using a rotating disk electrode (RDE) fitted with an analytical rotator MSRX (PINE Instruments, USA) coupled with the CHI 750A model work station. A conventional three electrode system with modified glassy carbon electrode (GCE) with a diameter of 3 mm as working electrode, a thin Pt wire as counter electrode and Ag/AgCl (sat. KCl) as reference electrode was used. Scanning electron microscopy (SEM) was performed by using a Hitachi S-3000H Scanning Electron Microscope. Attenuated reflectance spectroscopy (ATR) measurements were carried out using a Perkin-Elmer IR spectrometer. Powder X-ray diffraction (XRD) studies were performed in a XPERT-PRO (PANalytical B.V., The Netherlands) diffractometer using Cu Kα radiation ($k=1.54$ Å). Ultrasonicator DC150H (Taiwan Delta New Instrument Co. Ltd.) with operating frequency of 40 kHz and ultrasonic power output of 150 W has been used for sonication at room temperature.

2.2. Reagents and materials

Graphite powder with 98% purity and glucose oxidase, from *Aspergillus niger* were obtained from Sigma Aldrich. 0.1 M phosphate buffer solution (PBS) was prepared from 0.1 M Na_2PO_4 and NaH_2PO_4 in doubly distilled water and the pH was adjusted to 7. Inert atmosphere was set by passing N_2 over the solution during the electrochemical experiments. All the experiments were conducted at ambient temperature (25 ± 2 °C).

2.3. Fabrication of GCE/RGO–GOx modified electrode

Graphite oxide was synthesized from graphite by the modified Hummer's method (Hummers and Offeman, 1958; Guo et al., 2009; Wang et al., 2009b). The as-obtained graphite oxide was dispersed in water (0.5 mg/mL) and exfoliated by ultrasonication for 2 h to produce GO. Prior to electrode modification the GCE was polished with 0.05 μm alumina slurry and Buehler polishing cloth. It was then washed with deionized water and ultrasonicated for 3 min each in water and ethanol to remove any adsorbed alumina particles or dirt from the electrode surface and finally dried. RGO–GOx biocomposite was fabricated on the GCE surface by a one-step process. 40 μL of GO dispersion (0.5 mg/mL) and 60 μL of GOx solution (10 mg/mL in 0.1 M PBS, pH 7) were sonicated (30 min) in a vial to produce GO–GOx composite. Then, 10 μL of the GO–GOx composite (containing 2 μg of GO and 60 μg of GOx) was drop casted onto GCE and allowed to dry at room temperature and rinsed with deionized water to remove any loosely attached enzyme or GO particles. The GO–GOx modified electrode (GCE/GO–GOx) was transferred to N_2 saturated PBS (pH 5.0) solution. The GO in the GO–GOx film was then electrochemically reduced to RGO by performing continuous potential cycling (15 cycles) from 0 to −1.5 V (Guo et al., 2009) at a scan rate of 50 mV s^{-1}. The modified electrode is denoted as GCE/RGO–GOx.

3. Results and discussions

3.1. GOx immobilization and electrochemical reduction of GO to RGO by single step approach

Fig. 1 represents the electrochemical reduction process of GO. The cyclic voltammogram of the reduction process of GO on GCE is shown in the inset of Fig. 1. In the first cycle, a broad cathodic peak (I_{pc}) with an onset potential of −0.8 V was observed, attributed to the reduction of oxygen functionalities of GO (Guo et al., 2009). The reduction current decreases significantly in the consecutive cycles. The modified electrode is noted as GCE/RGO. It should be noted, GO has many reactive functional groups such as ketone, quinine, carboxylic acid, hydroxyl, etc. Upon dispersing GOx in GO solution, the GO functionalities at the edge planes can easily bind with the free amino groups of GOx through covalent linkage (Alwarappan et al., 2010a). Thus GOx is immobilized both by entrapment as well as by covalent linkage. Similarly, the as-prepared GO–GOx was electrochemically reduced in the same potential range and number of cycles. It can be seen form Fig. 1 that the immobilization of GOx on GO by entrapment and covalent linkage does not affect the characteristics of the electrochemical

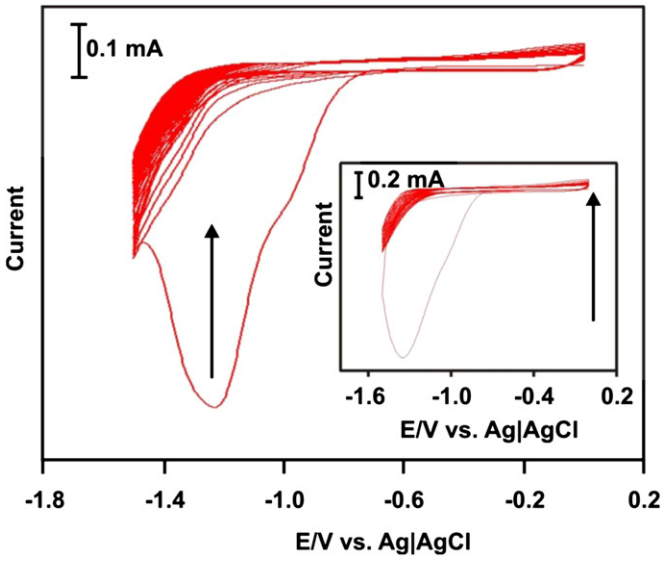

Fig. 1. Cyclic voltammogram of electrochemical reduction of GCE/GO–GOx to GCE/RGO–GOx in N_2 saturated PBS (pH 5). Scan rate: 0.05 Vs^{-1}. The inset shows the electrochemical reduction of GCE/GO under identical experimental conditions.

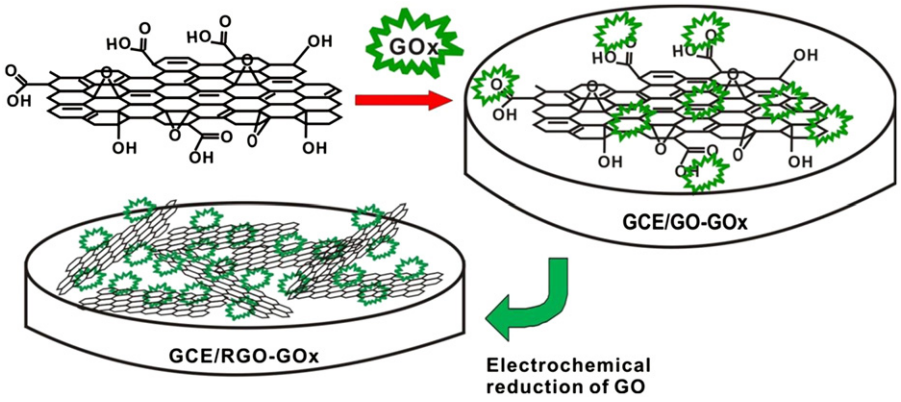

Scheme 1. Schematic representation of single-step fabrication of RGO–GOx biocomposite.

reduction process of GO. Relative to GO reduction, a significant decrease in the reduction peak current was observed during the first cycle of GO–GOx reduction. This could be due to the less availability of surface oxygen functionalities on GO, as they are covalently linked with the free amino groups of GOx as supported by the ATIR data. A similar immobilization of GOx on functionalized multiwalled carbon nanotubes has been reported earlier (Li et al., 2005). A schematic representation of GOx immobilization is given in Scheme 1.

3.2. ATR spectroscopy and X-ray diffraction studies

The conversion of graphite to GO produces different types of oxygen functionalities on the GO surface. ATR spectra in the infra red region can reveal the various functional groups by measuring the different types of bond vibrations. Fig. 2(A) shows the ATR spectra of GO, RGO and RGO–GOx composite. The spectrum of GO (curve a) exhibits a broad peak at 3400 cm^{-1} and a peak at 3230 cm^{-1}, ascribed to the O–H stretching vibrations of carboxylic acid group and intercalated water molecules (Kovtyukhova et al., 1999). Peak at 1630 cm^{-1} is due to the C=C skeletal vibrations of unoxidized graphitic domains. The C–OH stretching vibrations are found at 1230 cm^{-1}, while the C–O vibrations corresponding to epoxy or alkoxy groups are observed at 1058 cm^{-1}. The peak at 870 cm^{-1} is due to the epoxy groups in the GO (Jiang et al., 2012). When GO is electrochemically reduced to RGO (curve b) in pH 5, the intensity of the peak at 3400 cm^{-1} (O–H stretching) decreases, while the peak at 1230 cm^{-1} (C–OH stretching) almost disappears indicating the reduction of hydroxyl groups. Similar characteristic absorption peaks are also observed for RGO–GOx composite (curve c), revealing that the presence of GOx does not influence the electrochemical reduction process of GO. The peak corresponding to the carboxyl group around 1700 cm^{-1} is slightly shifted to lower wavenumber in the spectrum of RGO–GOx due to the formation of covalent linkage between the carboxylic group of RGO and the free amino group of GOx (Li et al., 2005). These observations indicate the formation of RGO–GOx composite. The surface morphological studies of the films by SEM also support the formation of RGO–GOx composite (see the supplementary material).

XRD patterns of GO and RGO are shown in Fig. 2(B). The exfoliated GO displays a sharp diffraction peak at 9.9°, attributed to the prevailing of AB stacking order as in graphite. However, no distinct sharp diffraction peaks were found in the XRD profile of RGO. Instead, a broad diffraction peak appears at 24° (Wang et al., 2009b), validating the efficient reduction of GO by the electrochemical method as reported elsewhere in literature (Guo et al., 2009).

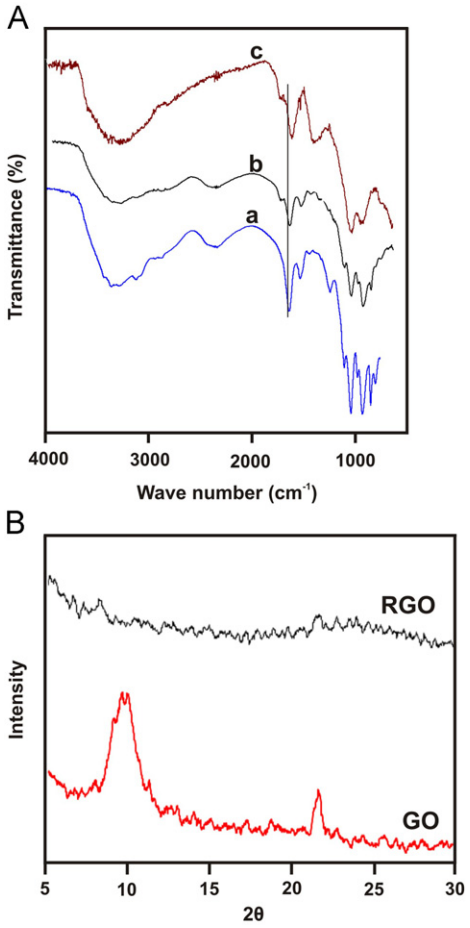

Fig. 2. (A) ATR spectra of (a) GO, (b) RGO and (c) RGO–GOx and (B) XRD spectra of GO and RGO.

3.3. Direct electrochemistry of GOx at RGO modified GCE

The direct electrochemistry of GOx at GCE/RGO has been studied by CV in N_2 saturated PBS (pH 7) at a scan rate of 50 m V s^{-1} in the potential range −0.7 to −0.1 V. To obtain the maximum possible direct electron transfer, GO to GOx ratio has been optimized by CV studies. We found that 2 μg GO to 60 μg GOx casted on GCE with surface area 0.07 cm^2 showed maximum redox peak currents for GOx. Hence, this optimized ratio (2 μg GO and 60 μg GOx) 1:30 was followed for all the experiments in

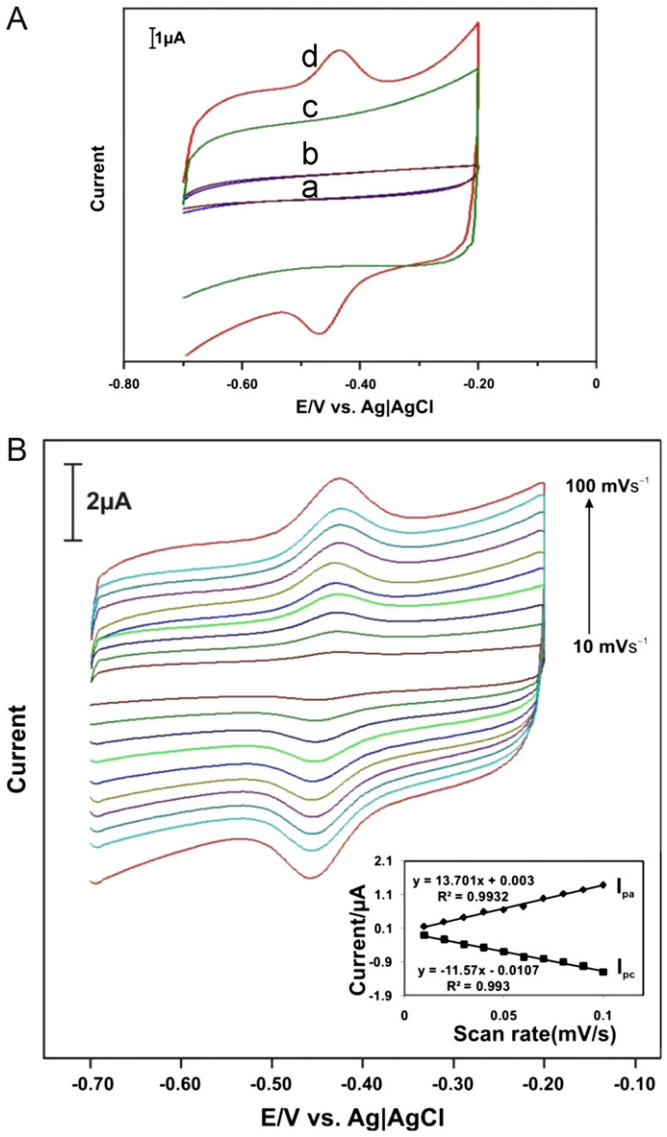

Fig. 3. (A) Cyclic voltammograms of (a) bare GCE, (b) GCE/GO–GOx, (c) GCE/RGO and (d) GCE/RGO–GOx in N_2 saturated PBS (pH 7). Scan rate: 0.05 Vs^{-1} and (B) cyclic voltammograms of GCE/RGO–GOx in N_2 saturated PBS (pH 7) at various scan rates: inner to outer are 10–100 m V s^{-1}. Inset to (B) shows the linear dependence of peak currents with scan rate.

this work. CVs were recorded for GCE/GO and bare GCE for comparison and are shown in Fig. 3(A). In the absence of GOx no peaks were obtained at bare GCE (curve a) or GCE/RGO (curve c). Also, GOx immobilized on GO does not show any peaks (curve b). Conversely, when the GO–GOx film is electrochemically reduced to RGO–GOx (curve d), GOx shows well defined redox couple with a peak to peak separation (ΔE_p) of 22 mV. The low ΔE_p value indicates a fast electron transfer process. The formal potential ($E^{\circ\prime}$) for the redox couple is −0.447 V which is close to the $E^{\circ\prime}$ values reported for GOx earlier (Shan et al., 2009; Durliat et al., 1988). This observation confirms the facile direct electron transfer from the redox site of the enzyme (FAD/$FADH_2$ redox center) to the electrode. The surface coverage concentration (Γ) of GOx at GCE/RGO–GOx modified electrode was calculated as 1.22×10^{-10} mol cm^{-2} using the equation, $\Gamma = Q/nFA$. Where Q is the charge (1.652×10^{-6} C), n is the number of electrons transferred ($n=2$), F is the Faraday constant (96,485.34 C mol^{-1}) and A is the GCE electrode area (0.07 cm^{-2}).

3.4. Effect of scan rate

The influence of scan rates on the cathodic and anodic peaks of GCE/RGO–GOx is shown in Fig. 3(B). The scan rates from inner to outer curves are 10, 20, 30, 40, 50, 60, 70, 80, 90 and 100 m V s^{-1}. Both anodic peak current (I_{pa}) and cathodic peak current (I_{pc}) increase linearly with the increase in scan rate from 10 to 100 m V s^{-1} which is characteristic of a surface-confined electrode process. The linear dependence of I_{pa} and I_{pc} on scan rate is given in the inset of Fig. 3(B). The linear regression equations for the redox process are written as $I_{pa}=13.701v+0.003$; $R^2=0.9932$ and $I_{pc}=-11.57v-0.0107$; $R^2=0.993$, where, v is the scan rate. The electron transfer rate constant (k_s) for GOx at GCE/RGO–GOx is calculated using the Laviron equation (Laviron, 1979) at higher scan rates.

$$\mathrm{Log}k_s = \alpha\,\mathrm{Log}(1-\alpha)+(1-\alpha)\mathrm{Log}\alpha-\mathrm{Log}(RT/nFv) \\ -\alpha(1-\alpha)nF\rightarrow E_p/(2.3RT) \quad (1)$$

where R is the universal gas constant (8.314 J mol^{-1} K^{-1}), T is the room temperature (298.15 K) and ΔE_p is the peak separation of the FAD/$FADH_2$ redox couple. Here, α value is assumed as ≈ 0.5 and the number of electrons transferred is considered as 2. The k_s value of GOx at GCE/RGO–GOx is calculated as 4.8 s^{-1} indicating fast electron transfer kinetics process.

3.5. Effect of pH

The effect of pH on FAD/$FADH_2$ redox couple of GOx at the RGO–GOx composite modified GCE have been studided. pH solutions 1, 4, 5, 7, 9, 11 and 13 were taken separately in different vials and the cyclic voltammograms were recorded for each pH. The solutions were purged with purified nitrogen gas for 15 min before recording CV. GOx exhibits steady redox peak currents over the investigated pH range. Both anodic peak potential (E_{pa}) and cathodic peak potential (E_{pc}) shifted to negative potentials with the increase in pH (Fig. S2). The influence of pH on $E^{\circ\prime}$ is given in the inset of Fig. S2. It is apparent from the plot that $E^{\circ\prime}$ shifts linearly with change in pH with a correlation coefficient of 0.9807. The slope value for the curve is −51.5 mV pH^{-1}, which is very close to the theoretical value of Nernstian equation for equal number of proton and electron transfer process.

3.6. Electrocatalytic activity of GCE/RGO–GOx towards glucose determination

The electrocatalytic activity of the RGO–GOx film towards glucose oxidation can be studied by observing the consumption of O_2 in PBS with the increase in concentration of glucose (Shan et al., 2009; Garjonyte and Malinauskas, 1999). During the oxidation of glucose, FAD is reduced to $FADH_2$ by accepting electrons from glucose. $FADH_2$ then reacts with O_2 to form H_2O_2 and FAD. Fig. 4 displays the cyclic voltammograms of GCE/RGO–GOx in oxygenated PBS at various concentrations of glucose. Upon addition of glucose, the oxidation peak current increases while the reduction peak current decreases significantly. The variation of I_{pc} with the concentration of glucose shows a linear relationship up to a certain limit (inset of Fig. 4). This can be attributed to the decrease in the O_2 content of the solution as it is consumed during the oxidation of glucose by the immobilized GOx as per the following equations (Wang, 2008):

$$\mathrm{GOx(FAD)}+\mathrm{Glucose}\rightarrow\mathrm{GOx(FADH_2)}+\mathrm{gluconolactone} \quad (2)$$

$$\mathrm{GOx(FADH_2)}+\mathrm{O_2}\rightarrow\mathrm{GOX(FAD)}+\mathrm{H_2O_2} \quad (3)$$

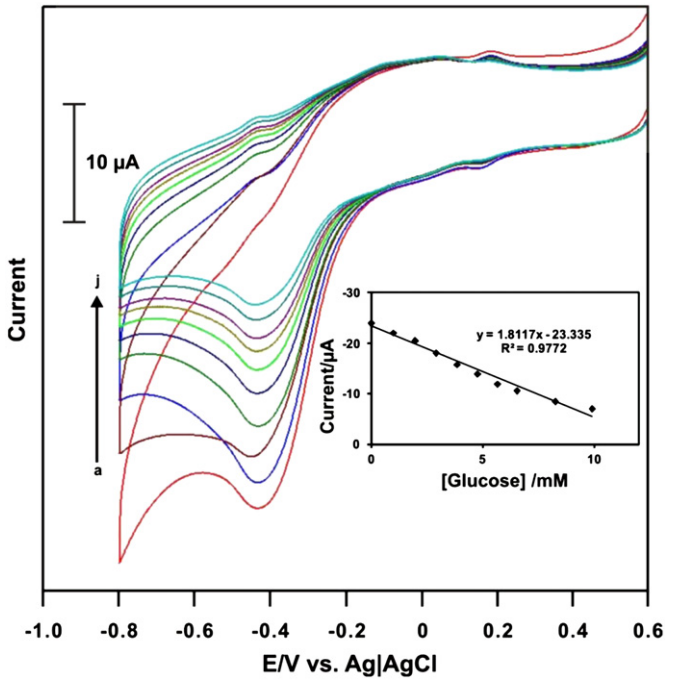

Fig. 4. Cyclic voltammograms of GCE/RGO–GOx in O_2 saturated PBS (pH 7) containing various concentrations of glucose (a) 0, (b) 0.99, (c) 1.96, (d) 2.91, (e) 3.85, (f) 4.76, (g) 5.66, (h) 6.54, (i) 8.26 and (j) 9.9 mM glucose. The inset shows the linear dependence of I_{pc} over glucose concentrations.

3.7. Amperometric determination of glucose at RGO–GOx modified electrode

Amperometry using rotating disk electrode (RDE) is a hydrodynamic electrochemical technique which involves the convective mass transport of reactants and products at the electrode surface, when the electrode is rotated at a specific speed (Bard and Faulkner, 2001). Fig. 5A shows the amperometric response of glucose at RGO–GOx modified RDE (area = 0.196 cm^2). It is notable, the amperometry was performed without any redox mediator and the electrode was rotated at a high speed of 3000 RPM, demonstrating the promising film stability. The performance of this glucose biosensor is based on the monitoring of amperometric responses produced by oxygen reduction upon increasing the concentration of glucose. When the reaction vessel was not properly covered and no oxygen atmosphere above the solution was maintained, the current decreased gradually even though glucose was not added (Fig. 5A(a)). This observation indicates that when the electrode is rotated at high rpm the O_2 content of the solution decreases gradually with time. Glucose solution was added at regular intervals of time (50 s). For every addition of glucose, a quick response (< 5 s) was observed and the peak current decreases. However, it can be seen from the enlarged view of the amperometric responses (Fig. 5A(b)) that the current drifts to a lower value after each addition. A sensing curve without drifting is more reliable. Therefore care has been taken to provide as much closed atmosphere as possible and O_2 atmosphere has been maintained above the solution which can overcome the problem of current drifting. Fig. 5A shows the amperometric response of glucose in properly covered reaction vessel with oxygen atmosphere maintained above the solution. With each glucose addition, the oxygen consumption increases and thus the catalytic current decreases. The curve is more stable this time. The linear dependence of the peak current with concentration of glucose is given in inset (c) to Fig. 5(A). RGO–GOx composite

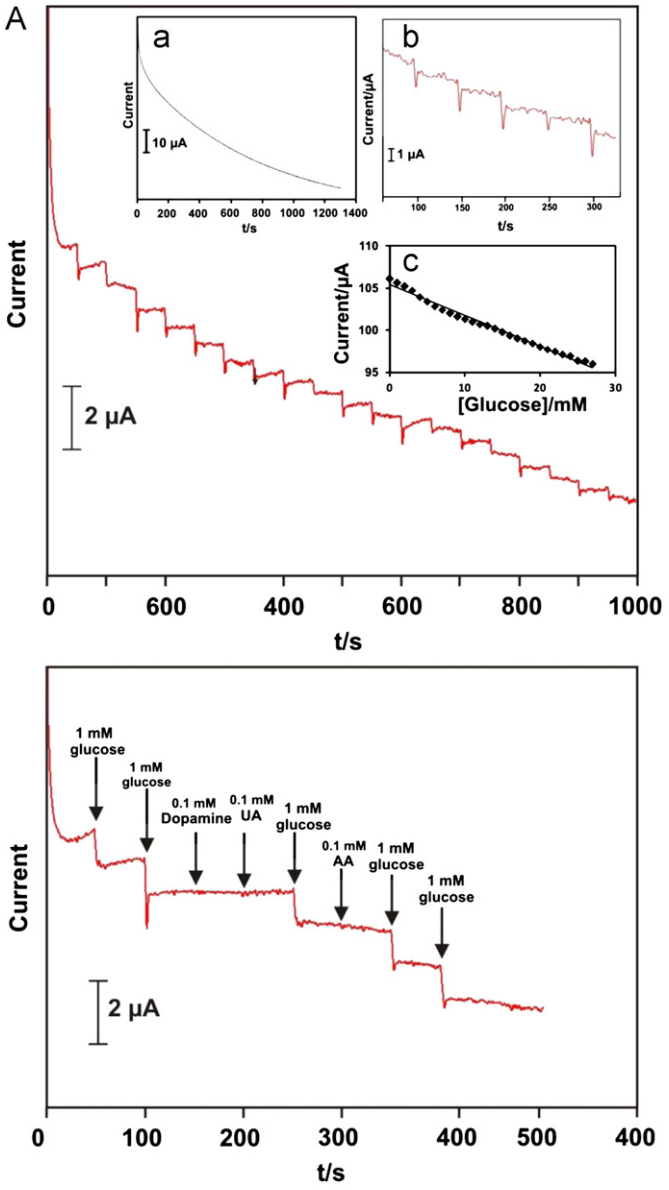

Fig. 5. (A) Amperometric *i–t* response of RGO–GOx modified rotating disk GCE for the addition of different glucose concentrations into O_2 saturated PBS (pH 7). Applied potential: −0.44 V and rotation rate: 3000 RPM. Inset (a) shows the enlarged view of the decrease in current with time in the absence of glucose. Inset (b) shows the amperometric response of glucose in the absence of a closed and O_2 atmosphere above the solution. Inset (c) is the plot of concentration of glucose vs current in the linear range. (B) Amperometric *i–t* response of RGO–GOx modified rotating disk GCE for the addition of various glucose concentrations followed by other common interfering species into O_2 saturated PBS (pH 7). Applied potential: −0.44 V and rotation rate: 3000 RPM.

modified RDE shows a steady state amperometric response in the range 0.1–27 mM of glucose. The linear regression equation is I_{pc} (μA) = 105.36 − 0.3634*C* (mM); R^2 = 0.988. The sensitivity of the RGO–GOx modified electrode is 1.85 μA mM^{-1} cm^{-2}. The wide working linear range of detection of this glucose sensor can be quite handy in practical applications. A comparison of analytical parameters of other electrodes is given in Table S1.

3.8. Selectivity, stability, reproducibility and repeatability of the biosensor

The selectivity of RGO–GOx film was evaluated in the presence of common interfering species such as dopamine, uric

acid, and ascorbic acid in oxygenated PBS. As shown in Fig. 5(B), for each addition of 1 mM glucose, the biosensor shows quick response. However, no noteworthy response was observed for the addition of 0.1 mM of dopamine, uric acid and ascorbic acid. Thus, GCE/RGO–GOx film is highly selective for glucose and it can be applied for glucose determination in human serum samples under physiological conditions. To understand the practical applicability of the biosensor, glucose determination in human serum has been conducted. The human serum was collected from a healthy person and the glucose content was pre-determined by a ROCHE COBAS C 111 ANALYZER. The glucose level was 4.198 mM. To determine the glucose content of the serum using the proposed sensor, 2 mL of the serum was diluted to 10 mL by adding PBS (pH 7). Then the glucose concentration was determined by the standard addition method. The concentration was calculated as 4.46 mM with a RSD of 4.9% for four measurements. The five times dilution was done to make sufficient volume of sample solution, so that RGO–GOx modified GCE (3 mm diameter), Ag/AgCl reference electrode and Pt wire auxiliary electrode could be comfortably accommodated.

To evaluate the storage stability of the biosensor, GCE/RGO–GOx was stored in PBS (pH 7) at 4 °C and the background current was recorded periodically by CV. After 20 days, the biosensor retained 93.4% of its initial response and 81% after 50 days, revealing its good stability. Such a high stability could be attributed to the good biocompatibility of the RGO and effective immobilization of GOx. Five individual electrodes were fabricated and their responses to 3 mM glucose in O_2 saturated PBS were measured under identical conditions. The relative standard deviation (RSD) of the response was 3.585%, which indicates that the fabrication method exhibits appreciable reproducibility. Similarly, to evaluate the repeatability of the biosensor, the RSD for six successive glucose determinations in different samples was obtained. In this process, the electrode was regenerated by immersing in PBS (pH 7) after each measurement. The biosensor displays acceptable repeatability with an RSD of 2.72%.

4. Conclusions

We demonstrated a simple and easy electrochemical approach for RGO–GOx biocomposite preparation. The GOx immobilization process is facile and does not involve any cross-linker. The wide linear range, fast electron transfer rate, high selectivity and the good stability of this sensor can extend its practical applications further. The performance of the biosensor has been accessed in mediator-free conditions with a sensitivity of 1.85 $\mu A\ mM^{-1}\ cm^{-2}$. The characterization of RGO–GOx by various methods suggests that the fabrication process mentioned in this work can be employed for a wide variety of biosensor and biofuel cell applications.

Acknowledgment

The authors express their gratitude to Veerappan Mani for his help in synthesis and characterization of graphene oxide and reduced graphene oxide. This project was supported by the National Science Council and the Ministry of Education of Taiwan (Republic of China).

Appendix A. Supplementary material

Supplementary data associated with this article can be found in the online version at http://dx.doi.org/10.1016/j.bios.2012.06.045.

References

Alwarappan, S., Erdem, A., Liu, C., Li, C.L., 2009. Journal of Physical Chemistry C 113, 8853–8857.
Alwarappan, S., Liu, C., Kumar, A., Li, C.Z., 2010a. Journal of Physical Chemistry C 114, 12920–12924.
Alwarappan, S., Joshi, R.K., Ram, M.K., Kumar, A., 2010b. Applied Physics Letters 96, 263702.
Baby, T.T., Aravind, S.S.J., Arockiadoss, T., Rakhi, R.B., Ramaprabhu, S., 2010. Sensors and Actuators B: Chemical 145, 71–77.
Bard, A.J., Faulkner, L.R., 2001. 2nd ed. John Wiley & Sons, Inc., 331.
Bharathi, S., Nogami, M., 2001. Analyst 126, 1919–1922.
Blin, J.L., Gerardin, C., Carteret, C., Rodehuser, L., Selve, C., Stebe, M.J., 2005. Chemistry of Materials 17, 1479–1486.
Cao, H., Zhu, Y., Tang, L., Yang, X., Li, C., 2008. Electroanalysis 20, 2223–2228.
Chen, Q., Kenausis, G.L., Heller, A., 1998. Journal of the American Chemical Society 120, 4582–4585.
Durliat, H., Barrau, M.B., Comtat, M., 1988. Bioelectrochemistry and Bioenergetics 19, 413–423.
Ekiz, F., Yuksel, M., Balan, A., Timur, S., Toppare, L., 2010. Macromolecular Bioscience, 1557–1565.
Fang, B., Zhang, C., Wang, G., Wang, M., Ji, Y., 2011. Sensors and Actuators B: Chemical 155, 304–310.
Foulds, N.C., Lowe, C.R., 1986. Journal of the Chemical Society—Faraday Transactions 82, 1259–1265.
Fu, Y., Li, P., Bu, L., Wang, T., Xie, Q., Chen, J., Yao, S., 2011. Analytical Chemistry 83, 6511–6517.
Garjonyte, R., Malinauskas, A., 1999. Sensors and Actuators B 56, 85–92.
Geim, A.K., Novoselov, K.S., 2007. Nature Materials 6, 183.
Gengler, R.Y.N., Veligura, A., Enotiadis, A., Diamanti, E.K., Gournis, D., Jozsa, C., Wees, B.J.V., Rudolf, P., 2010. Small 6, 35.
Guo, H.L., Wang, X.F., Qian, Q.Y., Wang, F.B., Xia, X.H., 2009. ACS Nano 3, 2653–2659.
Hummers, W.S., Offeman, R.E., 1958. Journal of the American Chemical Society 80, 1339.
Jia, W.Z., Wang, K., Zhu, Z.J., Song, H.T., Xia, X.H., 2007. Langmuir 23, 11896–11900.
Jiang, Y., Zhang, Q., Li, F., Niu, L., 2012. Sensors and Actuators B 161, 728–733.
Jody, L.H., Ellen, M.A., Ward, W.K., 2007. Journal of Diabetes Science and Technology 1, 18–27.
Kang, X., Wang, J., Wu, H., Aksay, I.A., Liu, J., Lin, Y., 2009. Biosensors and Bioelectronics 25, 901–905.
Kovtyukhova, N.I., Ollivier, P.J., Martin, B.R., Mallouk, T.R., Chizhik, S.A., Buzaneva, E.V., Gorchinskiy, A.D., 1999. Chemistry of Materials 11, 771–778.
Kuila, T., Bose, S., Khanra, P., Mishra, A.K., Kim, N.H., Lee, J.H., 2011. Biosensors and Bioelectronics 26, 4637–4648.
Laviron, E., 1979. Journal of Electroanalytical Chemistry 101, 19–28.
Li, J., Wang., Y.B., Qiu, J.D., Sun, D.C., Xia, X.H., 2005. Analytical and Bioanalytical Chemistry 383, 918–922.
Li, D., Muller, M.B., Gilje, S., Karner, R.B., Wallace, G.G., 2008. Nature Nanotechnology 3, 101–105.
Lin, Y., Lu, F., Tu, Y., Ren, Z., 2004. Nano Letters 4, 191–195.
Liu, L., Yu, D., Zeng, C., Miao, Z., Dai, L., 2010. Langmuir 26, 6158–6160.
Liu, S., Tian, J., Wang, L., Luo, Y., Lu, W., Sun, X., 2011. Biosensors and Bioelectronics 26, 4491–4496.
Novoselov, K.S., Geim, A.K., Morozov, S.V., Jiang, D., Zhang, Y., Dubonos, S.V., Grigorieva, I.V., Firsov, A.A., 2004. Science 306, 666–669.
Periasamy, A.P., Chang, Y.J., Chen, S.M., 2011. Bioelectrochemistry 80, 114–120.
Shan, C., Yang, H., Song, J., Han, D., Ivaska, A., Niu, L., 2009. Analytical Chemistry 81, 2378–2382.
Shen, J., Hu, Y., Shi, M., Lu, X., Qin, C., Li, C., Ye, M., 2009. Chemistry of Materials 21, 3514.
Song, P., Zhang, X., Sun, M., Cui, X., Lin, Y., 2012. RSC Advances 2, 1168–1173.
Wang, J., Musameh, M., 2003. Analyst 128, 1382–1385.
Wang, J., 2008. Chemical Reviews 108, 814–825.
Wang, Z., Zhou, X., Zhang, J., Boey, F., Zhang, H., 2009a. Journal of Physical Chemistry C 113, 14071–14075.
Wang, G., Shen, X., Yao, J., Park, J., 2009b. Carbon 47, 2049–2053.
Wu, P., Shao, Q., Hu, Y., Jin, J., Yin, Y., Zhang, H., Cai, C., 2010. Electrochimica Acta 55, 8606–8614.
Xian, C.G., Li, C.M., 2010. Physical Chemistry Chemical Physics 12, 12153–12159.
Yang, X., Hua, L., Gong, H., Tan, S.N., 2003. Analytica Chimica Acta 478, 67–75.
Yang, M.H., Choi, B.G., Park, H., Hong, W.H., Lee, S.Y., Park, T.J., 2010. Electroanalysis 22, 1223–1228.
Yin, H., Zhou, Y., Meng, X., Shang, K., Ai, S., 2011. Biosensors and Bioelectronics 30, 112–117.
Zhou, K., Zhu, Y., Yang, X., Li, C., 2010. Electroanalysis 22, 259–264.